IEEE Access
Multidisciplinary | Rapid Review | Open Access Journal

Received March 19, 2021, accepted April 6, 2021, date of publication May 4, 2021, date of current version May 20, 2021.

Digital Object Identifier 10.1109/ACCESS.2021.3077531

Increasing Electric Vehicle Autonomy Using a Photovoltaic System Controlled by Particle Swarm Optimization

HABIB KRAIEM[1], AYMEN FLAH[2], NAOUI MOHAMED[2], MAJED ALOWAIDI[3], (Member, IEEE), MOHIT BAJAJ[4], (Member, IEEE), SHAILENDRA MISHRA[5], (Senior Member, IEEE), NAVEEN KUMAR SHARMA[6], (Senior Member, IEEE), AND SUNIL KUMAR SHARMA[3]

[1]Department of Electrical Engineering, College Engineering, Northern Border University, Arar 73222, Saudi Arabia
[2]PEESE, National School of Engineering of Gabès, University of Gabès, Gabès 6029, Tunisia
[3]Department of Information Technology, College of Computer and Information Sciences, Majmaah University, Al Majma'ah 11952, Saudi Arabia
[4]Department of Electrical and Electronics Engineering, National Institute of Technology Delhi, New Delhi 110040, India
[5]Department of Computer Engineering, College of Computer and Information Sciences, Majmaah University, Al Majma'ah 11952, Saudi Arabia
[6]Department of Electrical Engineering, I. K. Gujral Punjab Technical University, Jalandhar 144603, India

Corresponding author: Sunil Kumar Sharma (s.sharma@mu.edu.sa)

The work of Majed Alowaidi was supported by the Deanship of Scientific Research at Majmaah University under Project R-2021-109.

ABSTRACT A photovoltaic-powered electric vehicle is a complex system that necessitates the use of a high-performance control algorithm. This paper aims to boost the performance of a photovoltaic system by employing a suitable algorithm to control the power interface. The main goal is to find an effective and optimal control law that will enable the photovoltaic generator (GPV) to generate the maximum amount of power possible. The main facts dealt with in this article are the mathematical simulation of the photovoltaic system, its function, and its characteristics, considering the synthesis of the step-up converter and the analysis of the maximum power point tracking algorithm. This study examines and compares two control techniques for extracting full power from the solar energy system. These two techniques are the classical ''perturbation and observation'' (P&O) method and the intelligent solution ''particle swarm optimization (PSO) method.'' The PSO solution is tested for two versions: the online PSO version and the table PSO version. The Simulink/MATLAB tool is used for simulation and comparative experiments based on the performance metrics provided. The study revealed that smart technology delivers improved efficiency than the classic edition.

INDEX TERMS Battery state of charge, electric vehicle, maximum power point tracking, perturb & observe, particle swarm optimization, photovoltaic system.

LIST OF SYMBOLS

K_t	Temperature coefficient
G	Irradiation factor
G_{ref}	Reference irradiation
T_c	actual cell temperature
T_{ref}	nominal operating temperature
I_d	Diode current
I_{RP}	Shunt current
R_{se}	Serial resistance
I_{cel}	Cell current
I_p	Load current
N_p	Parallel cell number
N_s	Serial cell number
I_{ph}	photocurrent
V_{out}	Output voltage from chopper
v	Capacity voltage
$V_{b/cell}$	Voltage by the cell in the battery
N_{pl}	Battery cells parallel number
N_{si}	Battery cells serial number
SOC	State of charge
S_{ocm}	Maximum of SOC
V_b	Battery voltage
I_b	Battery current

The associate editor coordinating the review of this manuscript and approving it for publication was Alon Kuperman.

R_{lt} Electrochemical resistance
C_{lt} Electrochemical capacitance
V_{oc} Open circuit voltage
D Dutty cycle

I. INTRODUCTION

Nowadays, solar energy technology has evolved exponentially due to the steady streaming of sunlight across the world. This alternative energy source decreases air emissions and reduces the pollution created by conventional energy industries. The generation of electricity from this source is very feasible for a variety of different applications. The rapid production of solar energy instruments and the current, complete kit has steadily appeared in the field of EVs. The creation of a solar electric vehicle and numerous implementations have been revealed and presented in the literature [1], [2].

Researchers in [3] have provided the possibility of covering the surface of EVs with photovoltaic cells to store a large amount of energy in the battery system.

Similarly, in [4] and researchers used the dual induction machine to supply the vehicle with the necessary torque, and then used the photovoltaic system with the battery system to deliver the engine with the required electrical energy [5], [6].

There is an essential space on the vehicle where the photovoltaic cells can be placed. This is can improve the overall vehicle autonomy if correctly managing these photovoltaic sources. Table (1) exposes the possible free area that can be used for inserting photovoltaic cells for three kinds of vehicles. Also, an approximation of the obtained power is made at the end of this study to show the vehicle size's efficiency on the obtained power.

TABLE 1. Three kinds of vehicle and their possible free spaces for inserting photovoltaic cells *.

Vehicle Model	*Audi R8*	*Range Rover*	*Commercial Truck*
Right side (m^2)	0.83	0.05	23.86
Left side (m^2)	0.83	0.05	23.86
Topside (m^2)	2.27	1.06	15.88
Rear side (m^2)	0.6	0.03	4.2
Total (m^2)	4.53	1.19	67.8
Polycrystalline Solar cell M3 153.4 mm*153.4 mm			
Number of cells	151	40	2260
Given power	664.4 (W)	176 (W)	9944 (W)

**These statistics are taken from SolidWorks software, and vehicle models were taken from the database GrabCAD.com.*

Referring to table (1), it is clear that a large space is exposed to solar if the vehicle is outside. This free space can be a benefit if used as a support for placing a photovoltaic cell. These statistics don't take into consideration the glasses-free space. For example, the Audi R8 car can have a maximum of 664.4 W from solar. This is if using the M3 PV cells, where each particle can give 4.4 W.

For the same example, the R8 maximum power can be valued as 650 hp, equivalent to 430 KW; this is for the highest possible speed, which can touch 350 km/h. For the lowest speeds, at 50 km/h, the car will consume 60 kW as maximal power, and the PV system here can help by 1% in the best of cases.

For commercial trucks, this system can be more beneficial as there is a large free space that can be used for generating solar energy. The needed horsepower for a commercial truck is between 400 and 550, equivalent to 298 to 410 kW as the maximum possible given power. Here, the PV system can help by 2% for the maximum truck conditions long road if all cells are used. However, this is the case on-road or into the city. The method estimation of the energy gain is difficult as this depends on the vehicle position face the solar rays and depends on the existing obstacles on the road. This makes extracting the maximum of energy in all these conditions very difficult as the car can move from a situation to another rapidly.

Basing on this special phenomenon, this work was proposed. It can be classified as a problem of extracting the maximum of energy from solar radiation and storing it into a battery system for future use. If inserted into an electric vehicle, this solution will facilitate its autonomy and help resolve the problem of vehicle recharge time.

A. PROBLEMS AND SOLUTIONS

The key issue with a solar-powered system is climate change, which applies to changes in irradiation. This affects the energy viability of the PV system. To solve the problem, researchers have introduced a variety of software applications that can obtain the optimum energy for various weather conditions.

The MPPT "Maximum Power Point Tracking" control comes as a necessary control loop to extract the maximum of power from the photovoltaic system [7], [8]. This technology was developed in 1968 and had an essential role in the operation of the panel. In the literature, several methods have been developed on the MPPT algorithm to improve the global performance of this energy source. The conventional method was based on the principle of the incremental conductance method (IC) [9]. The principle is based on the PV generator conductance derivative to know the relative position of the MPP, which allows applying a control action adequate to pursuing MPP.

Other researches were concentrated on the Perturb and Observe method (*P&O*). It is widely used due to its simplicity and ease to use. The main advantage of this algorithm is the simple control structure and the reduced number of measured parameters, but it presents a big problem regarding the chattering's on the given power form [10], [11].

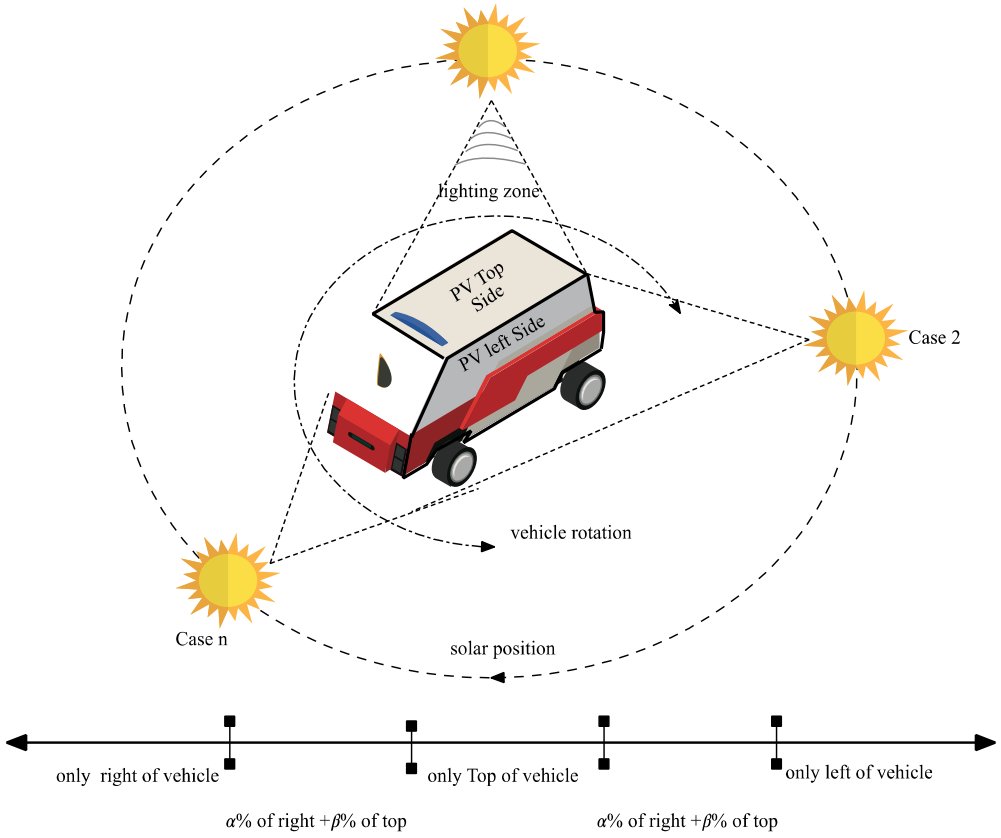

FIGURE 1. Sunshine and vehicle position.

Based on [7], the authors proved that those algorithms are incapable of tracking the MPP of solar radiation are changing rapidly. Also, under partial shade conditions, these algorithms cannot operate the system at the MPP.

In the same field, other techniques have been exposed based on intelligent optimization, such as the fuzzy logic method and the neural network method are used in applications to improve the energy efficiency of this system. The two methods give a good result, but the big problem is the required database for adjusting these algorithms [12].

Particle Swarm Optimization (PSO) is an algorithm inspired by the social behaviour of animals that evolve in groups (e.g., birds). Indeed, we can observe relatively complex movement dynamics in these animals. Each individual has a limited "intelligence" and has only local knowledge of its position in the swarm [13]. The PSO algorithm is widely used to improve overall performance. The PSO algorithm is widely used to improve overall performance, and it has proven its effectiveness in solving the problem mentioned above.

B. PROBLEM FORMULATION

If concentrating on the urban electric vehicle, it is clear that the car can't always be exposed to direct solar rays. Its position faces buildings, trees, or clouds affect the value of luminosity applied on the vehicle surface. Actually, in the traditional photovoltaic systems, as in the case of isolated PV stations for feeding isolate loads, the radiation variation doesn't cause a real problem as this is on all day, and the variation is very slow. But for the case of a vehicle that has a PV cell on the vehicle body, this is very different. This because of the vehicle speed and the rapid movement from a situation to another [14]. Figure (1) describes this problem and shows that the vehicle is making a transition between the shadow areas and the light areas. The rapid transition from these situations causes a problem for extracting the maximum power from the photovoltaic cells at the right moment.

To maximize the energy performance and make this energy source more efficient for a vehicle in an urban zone, this paper searches for an optimal control method that can be applied to improve the total energy efficiency and then increase vehicle autonomy. Therefore, this work-study a useful solution basing on intelligent algorithms and have the principle of bird movement for touching the desired goal. This technique is called the Particle Swarm Optimization (PSO) algorithm. It can be classified as an optimization problem resolving tool. It shows its efficiency in various problems as it is in [15] which search optimize the PI controllers for having better performances.

In the main part of the photovoltaic control tool, the classical P&O approach has been used, and the major focus of the current solution is based on it. Therefore, in order to validate the efficacy of the suggested solution, a distinction is made at

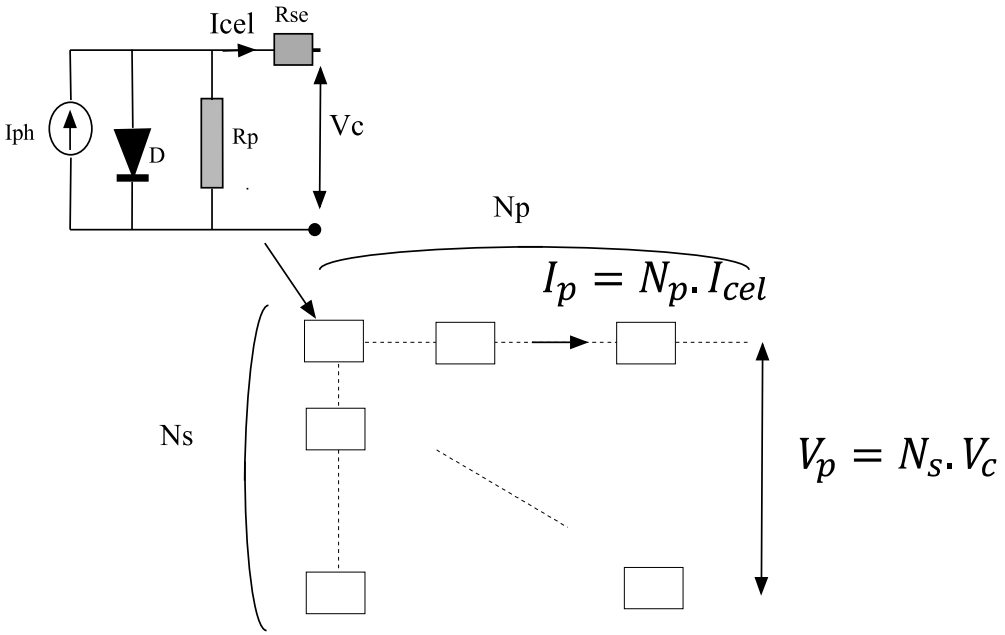

FIGURE 2. Equivalent model of a photovoltaic cell into a panel.

the conclusion of this paper between the energetic efficiency of the two methods to make recommendations for the right method in this situation.

So, based on this objective, this paper is organized into six sections. After a general introduction, which describes the paper context and explains the problem that needs resolving, the PV panel and their detailed mathematical model is exposed. As the boost DC/DC converter is used, the next section described it by giving its corresponding model. Then, the MPPT controller and the P&O-MPPT and PSO-MPPT algorithms are explained and theatrically compared.

Before the conclusion, the paper exposes the simulation results for each case and gives a detailed discussion.

II. PHOTOVOLTAIC GENERATOR

This study concentrates on the photovoltaic system. This part describes the mathematical equations of this generator.

This is by supposing that the photovoltaic cell has a behaviour equivalent to a current source proportional to the current generated by the illumination of the cell. The model is complemented by a "R_{se}" serial resistor represents the contact and connection resistor, and an "R_p" shunt resistor represents the leakage current at the junction. Figure (2) shows the equivalent diagram of a photovoltaic panel based on "N_s" and "N_p" cells, serial and parallel, respectively.

"I_{cel}" designs the output current from the cell. It can be calculated based on equation (1). "I_D" is the current inside the diode, and "I_{Rp}" is the current inside the parallel resistance. "I_{ph}" is called photocurrent generated by the influence of solar irradiation and cell's temperature, and it can be estimated as it is in equation (2) [7], [16], [17].

$$I_{cel} = I_{ph} - I_d - I_{Rp} \tag{1}$$

$$I_{ph} = \frac{G}{G_{ref}}\left(I_{ph,ref} + K_t\left(T_c - T_{ref}\right)\right) \tag{2}$$

In this equation, "K_t" is the Temperature coefficient of the short circuit "G" is the irradiance factor, and "G_{ref}" is the reference irradiance at standard operating conditions. "T_c" is the actual cell temperature, and "T_{ref}" is the nominal operating temperature equal to 25°C.

As the semiconductor diode is a nonlinear device, its proportional equation can be depicted from the current expression in equation (3).

$$I_d = I_s e^{\left(q\frac{V_D}{(n.k.T_C)} - 1\right)} \tag{3}$$

where "I_s" is the reverse saturation current, which is variable with temperature as it is described in [18]. "k" is the Boltzmann constant, and "n" is the ideality factor of the diode. "T_C" is the cell temperature. "V_D" represents the diode voltage.

Since the voltage of the parallel load is always the same, it is possible to indicate that $V_D = V_{RP}$ and the Shunt current noted "I_{RP}" could be represented by equation (4).

$$I_{RP} = V_c + R_{se}.I_{cel} \tag{4}$$

Based on the previous equations, the new expression of the load current can be expressed in equation (5).

$$I_p = N_p I_{ph} - N_p I_s\left(e^{\frac{q}{n.k.Tc}\left(\frac{V_p}{N_s} + \frac{R_{se}I_p}{N_p}\right)} - 1\right) - \frac{N_p}{R_p}\left(\frac{V_p}{N_s} + \frac{R_{se}I_p}{N_p}\right) \tag{5}$$

Basing on these equations, the characteristics of a photovoltaic panel, which has 37.8 V as a voltage and a short circuit current equivalent to 8.25 A, can be shown in figure (3). This is for serial resistance equivalent to 0.001 Ω and a parallel resistance equivalent to 1 KΩ. So this will give an electrical power equal to 250 W for the nominal condition related to 25 °C as temperature and 1000 W/m^2 as a luminosity factor.

III. DC/DC CONVERTER

Here, the role of the DC/DC converter is to adapt the photovoltaic source power and the load for assuring a maximum power transfer under any operating conditions.

This electronic system is a static converter used to generate a variable DC voltage from a fixed voltage source. It consists of capacitors, inductors, and switches. All these devices do not consume any power in the ideal case, and they can be neglected in real applications. This specification gives this converter good efficiency. In the major of cases, the principle used switch inside this converter is based on a MOSFET transistor. As it gives a large scale of power variation but has minimal dissipated power. If the switch is blocked, its current is zero, so it does not dissipate any power; if it is saturated, the voltage drop across its terminals will be almost zero, and therefore the power loss will be very small.

This switcher is controlled by a PWM (Pulse Width Modulation) signal, which has a fixed frequency and a variable duty cycle noted "D."

Various versions exist having the same specification of this converter, as the "buck converter," "boost converter," and "buck-boost converter." Figure (4) gives a general view of these DC/DC converters with their standard forms.

Concentrating on the step-up converter, which is used for increasing the voltage from the photovoltaic generator. We, not the output voltage by V_{out} and the inputted voltage, from the PV generator, by V_{in} [19], [20].

From the other side, as there are two situations for the used transistor, the dynamic model of the Boost converter has two different models, and the power flow will be controlled by adjusting the ON/ OFF position of the transistor.

Basing on Kirchhoff's laws, it is possible to indicate that when K = 1, the switch is ON. The equations can be written as it is in equation (6).

$$if\ (ON\ or\ u=1)\ then \begin{pmatrix} L\dfrac{di}{dt} = E \\ C\dfrac{dv}{dt} = -\frac{v}{R} \end{pmatrix} \tag{6}$$

When K = 0, the switch is OFF, the equations can be written as it is in equation (7).

$$if\ \ (\text{OFF or u} = 0)\ then \begin{pmatrix} L\dfrac{di}{dt} = -v + E \\ C\dfrac{dv}{dt} = i - \dfrac{v}{R} \end{pmatrix} \tag{7}$$

A bilinear equation then is described for this converter. Equation (8), describes this relationship. "u " is a "1" for the ON and "0" for the OFF switcher situation [21].

$$\begin{bmatrix} \dfrac{di}{dt} \\ \dfrac{dv}{dt} \end{bmatrix} = \begin{bmatrix} \dfrac{-(1-u)}{L} & 0 \\ \dfrac{-1}{CR} & \dfrac{(1-u)}{C} \end{bmatrix} \begin{bmatrix} v \\ i \end{bmatrix} + \begin{bmatrix} \dfrac{E}{L} \\ 0 \end{bmatrix} \tag{8}$$

$$\begin{bmatrix} \dot{E} \\ \dot{i} \\ \dot{v} \end{bmatrix} = \begin{bmatrix} \dfrac{1}{C_{in}}\left(i_{c_{in}}\right) \\ \dfrac{1}{L}(E-v) \\ \dfrac{1}{C}(i-i_{out}) \end{bmatrix} + \begin{bmatrix} 0 \\ \dfrac{1}{L}v \\ -\dfrac{1}{C}i \end{bmatrix}.u \tag{9}$$

From the other side, some versions add an initial capacity in parallel to the photovoltaic generator to reduce the voltage variation for this generator. So, take into consideration this capacity (noted C_{in}), the dynamic model of the boost converter can be expressed as it is in equation (9). "$i_{c_{in}}$" represents the current inside the initial capacity "C_{in}" "i_{out}" represents the outputted current.

Another equation is important too, in it describes the relationship between the input and the outputted voltage, basing the duty cycle factor, noted D. Equation (10), shows it.

$$v = \frac{1}{1-D}.E \tag{10}$$

IV. BATTERY MODEL

As the photovoltaic generator is used for charging a battery pack, it necessary to know the Mathematical battery model and make it understandable.

In equation (11), we show the battery output voltage, referred to as "V_b" by one cell. Ultimately, the voltage expression depends on the "V_{oc}" which is the open-circuit voltage. "R_b" is a cell's ohmic resistance. "R_{st}" and "C_{st}" are the resistance and capacitance of the electromagnetic short-term double-layer properties, respectively, and "R_{lt}" and "C_{lt}" are the resistances and capacitances of the electrochemical long-time-interval mass transport effects.

$\ll I_b \gg$ is the cell load current. As this element can be discharged or charged, $\ll I_{st} \gg$ will be positive or negative, respectively [22].

$$V_{b/cell} = V_{oc} + R_b I_b + \int \frac{I_b - \frac{V_{st}}{R_{st}}}{C_{st}} dt + \int \frac{I_b - \frac{V_{lt}}{R_{lt}}}{C_{lt}} dt \tag{11}$$

The battery pack voltage "V_b" depends on the number of serial and parallel of used cells. Equation (13), explains that relation. The battery resistance can also be found in equation (12). We indicate by "R_o", the battery cell charging or discharging resistance.

$$R_b N_{pl} = \left(R_o + R_{st} * {}^{I_{st}}\!/_{I_l} + R_{lt} * {}^{I_{lt}}\!/_{I}\right) N_{si} \tag{12}$$

$$N_{pl} V_b = N_{sl} V_{b_{/cell}} \tag{13}$$

The battery state of charge SOC can be expressed in function of time as it is in equation (14). We note "W" the charge/discharge coefficient, "N" is the stands of the

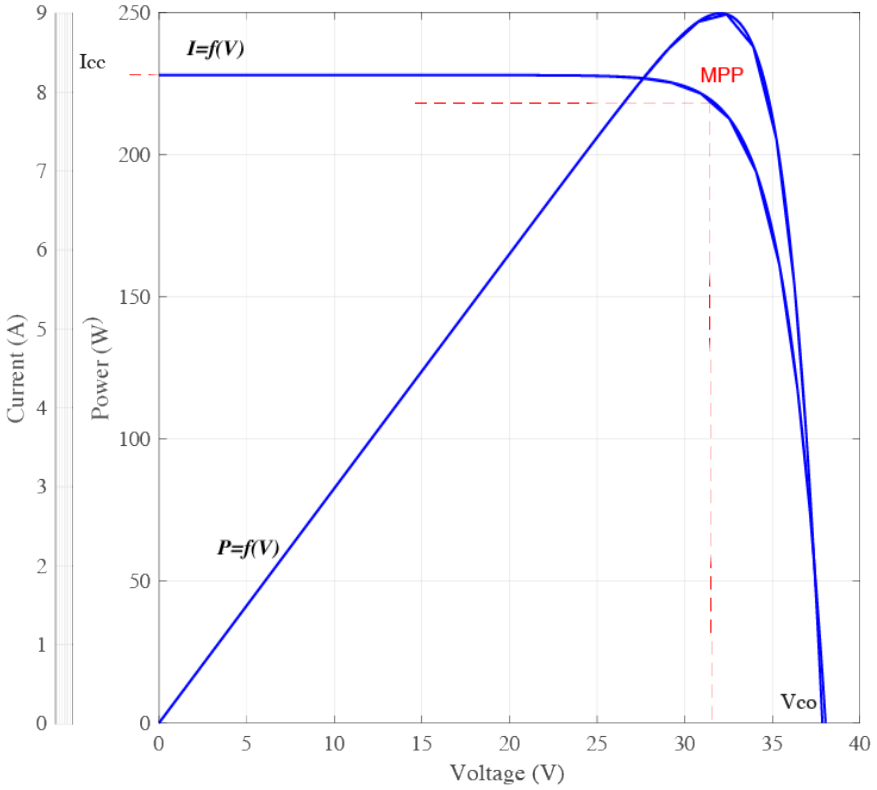

FIGURE 3. I-V and P-V characteristic curves at a fixed irradiation and temperature (G = 1000W/m∗m, 25°C).

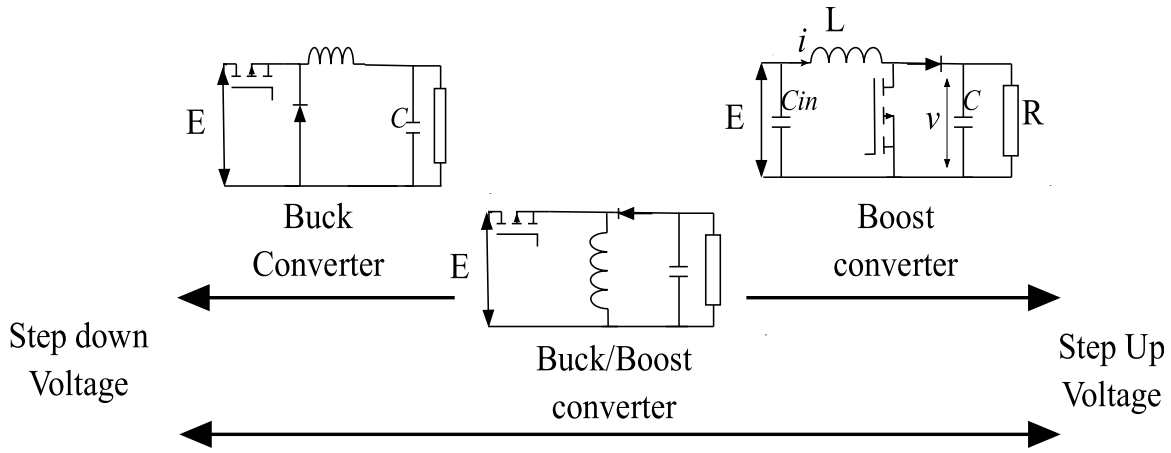

FIGURE 4. DC/DC converters designs.

battery self-discharge. "*SOC*" is the maximum state of charge [23]–[25].

$$SOC\ (t) = \int_{t-1}^{t} \frac{W\ (V_b.I_b)}{60.S_{ocm}} - \frac{SOC\ (t-1)\ .N}{60} dt \quad (14)$$

V. THE MPPT CONTROL TECHNIQUE

The main drawbacks faced by the PV system are that the sun's irradiance is rarely constant, and It is, therefore, impossible to maintain the full production from the panel. Therefore, when any source differs, it is always easier to operate on the current output obtained and modify it dynamically so that the output stays unchanged due to the loss on the input side. This is exactly what the MPPT is doing. Full Power Point Tracking is digitally controlled. The boost converter outputted voltage looks at the terminal of the PV system and applies it to the voltage of the battery. It then indicates what the right power that the panel can use to charge the

battery is. This is transformed to the right voltage to provide the full current to the battery. For doing this, various algorithms and technique were exposed to literature, and the P&O technique is the basic version, which is largely used due to its algorithm simplicity. But for fast changes that occur on the environmental condition, the efficiency of this technique decrease. This specification is largely frequent in the studied system. Intelligent technique, thus, with the definition of the optimization problem solved, was proposed as a PSO algorithm. This section discusses the distinction between these two algorithms and their interior designs.

A. P&O-BASED MPPT TECHNIQUE

The P&O approach is the most widely used in MPPT testing since it is very basic and convenient to use. Only panel voltage and current measurements E and I are needed to obey the maximum power point in the event of changes in irradiation and temperature [10], [11], [26].

The P&O system operates by regularly disrupting the E-panel voltage with the LV and by monitoring the difference of the electrical energy supplied at the PV output.

- If $\Delta P > 0$, the voltage perturbation is closer to the operating point of the MPP, and the voltage continues to be perturbated in the same direction, which will move the operating point until the MPP is reached.
- If $\Delta P < 0$, the operating point moves away from the MPP, and the voltage will be perturbed by the algebraic sign, which is opposite to the previous sign, to move the operating point until the MPP is reached.

The theory of this algorithm can be modelled by a flowchart, as seen in Figure 5.

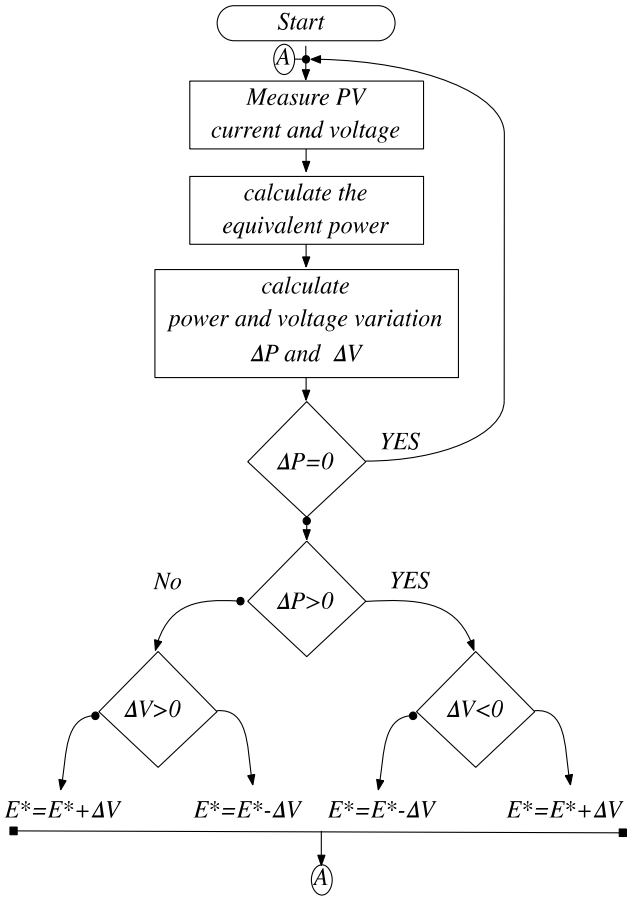

FIGURE 5. P&O organization.

B. PSO-BASED MPPT TECHNIQUE

Inspired by the social actions of animals that develop into groups, the concept of the PSO algorithm is suggested.

In fact, we can observe relatively complex dynamics of movement in these species. Each person has a small "intelligence" and has only local knowledge of his place in the swarm [27], The swarm of particles corresponds to a group of simple agents, called particles. The particle is thought to be a solution to the problem of position and velocity. In addition, each particle has a memory to remember its best performance, noted "*pbest*" and the group best performances obtained, noted "*gbest*". All these particles search to guarantee the objective function, which searches increasing the output PV power to the maximum value as it is indicated in equation (15).

$$P\left(d_i^k\right) - P\left(d_i^{k-1}\right) > 0 \tag{15}$$

The movement of a particle is influenced by three factors.

- A component of inertia: the particle tends to follow its current direction of movement.
- A cognitive component: the particle tends to go to the best site it has already passed through.
- A social component: the particle tends to rely on the experience of its congeners and, thus, to move towards the best site already reached by the other particles.

The expression that connects the three components is in equation (16).

$$v_i^{k+1} = w.v_i^k + c_1.r_1.(pbest_i - x_i^k) + c_2.r_2.(gbest_i - x_i^k) \tag{16}$$

The movements of the particles are based on (17), which is the same formula for adjusting the duty cycle position.

$$x_i^{k+1} = x_i^k + v_i^{k+1} \tag{17}$$

where: v_i is the current velocity of particle i at iteration, $x_i(t)$ is the current position of particle i. w is the inertia weight, c_1, and c_2 are the acceleration constants, p_{best} and g_{best} are the best local and best global position. r_1 and r_2 are random numbers between 0 and 1. The algorithm principle is exposed in figure (5).

It is important to indicate that $i \in [\,1\ N_p\,]$, N_p is the number of the particle.

For this method, the duty cycle expression for each particle "i" is calculated using a new formula as it in equation (18) if $\Delta P > 0$, and (19) if $\Delta P < 0$. We note P_{mpp}^k the

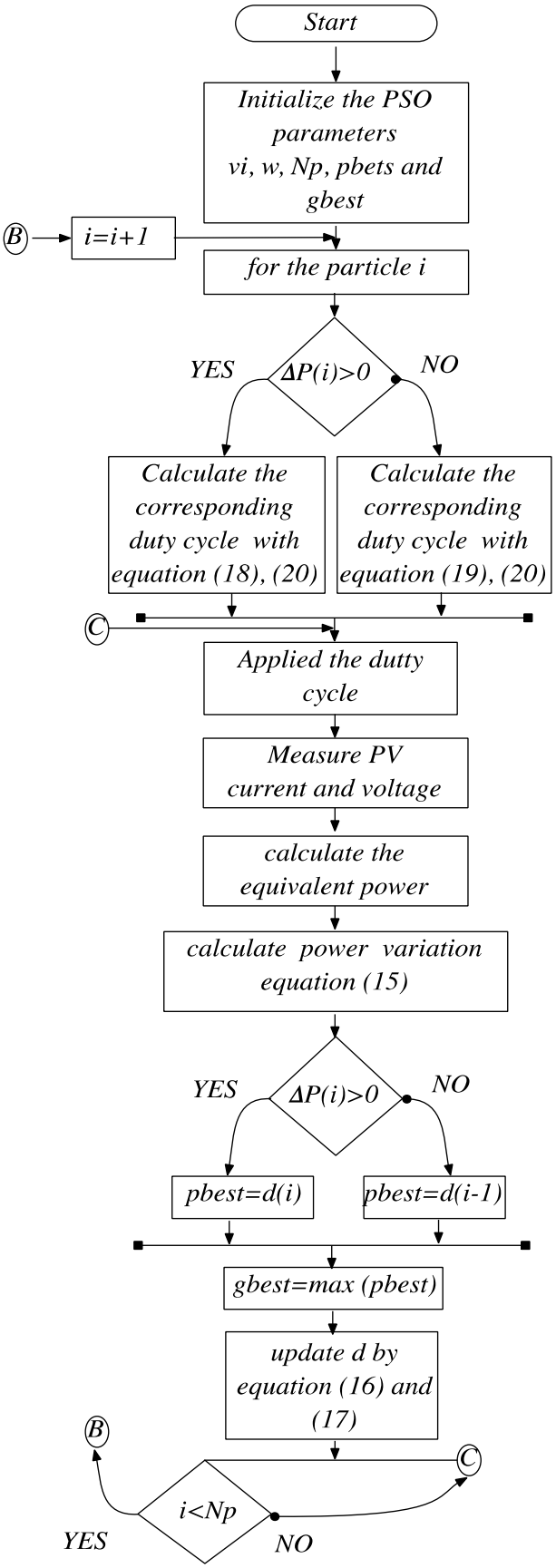

FIGURE 6. PSO-MPPT organization.

actual array maximum power and $gbest^k$, the corresponding duty cycle.

$$d^{k+1} = gbest^{k+1} = gbest^k - \frac{1}{\left(P^k_{mpp} - P^{k-1}_{mpp}\right)/\triangle d}\left(P^{k-1}_{mpp} - P^k_{mpp}\right) \quad (18)$$

$$d^{k+1} = gbest^{k+1} = gbest^k - \frac{2}{\left(P^k_{mpp} - P^{k-1}_{mpp}\right)/\triangle d}\left(P^{k-1}_{mpp} - P^k_{mpp}\right) \quad (19)$$

The new obtained duty cycle will be then perturbed in two different directions, by adding and reducing a constant value noted ε from the first and the last particle position. This is explained in equation (20).

$$d^{k+1}_i = \left[d^k_1 + \varepsilon, d^k_2, \cdots, d^k_{Np-1}, d^k_{Np} - \varepsilon\right] \quad (20)$$

The value of ε is generally fixed from the initial iteration, it is selected to control the fluctuation of power on the PV array. We note that this technique is recommended for $Np => 3$. It is possible to adjust ε, by controlling the operating voltage. The marge of variation of ε is at it is in equation (21).

$$0 < \varepsilon < 1 \quad (21)$$

VI. RESULTS AND DISCUSSION

In this section, we try to analyze the obtained results. As it is indicated before, the two control methods P&O-MPPT and PSO-MPPT will be compared to define the best solution for the cited problem.

The MATLAB Simulink tool was used to simulate the general system function. The simulation conditions are related to the constant temperature, which is equal to 25°C, the marge of irradiation factor is included between [$\mathbf{400}\frac{W}{m^2}$, $1000\frac{W}{m^2}$]. For the other parameters related to the PV system and the PSO parameters, table (2), summarize them.

The simulation phase was divided into two parts. The first one is related to the P&O-MPPT technique application and its results. The second part of this section is designed for showing the PSO-MPPT results. This is by giving and irradiation form as it is in figure (7).

The given power under these conditions will be varied between 2 KW and 6 KW, for the worst and the better irradiation factor consequently.

A. MPPT-P&O CONTROL SIMULATION RESULTS

The previous irradiation form is used for verified the results of the MPPT technique if using the P&O control solution. The non-stability of the given power can be verified by the fluctuation on the duty cycle parameter related to the P&O algorithm running principle. The fixed step of the duty cycle influences the overall algorithm precision. This is proved in this reference [28]. So figures (8) and (9) show the obtained results if using this method. These results were depicted for a duty cycle variation as it is in figure (8).

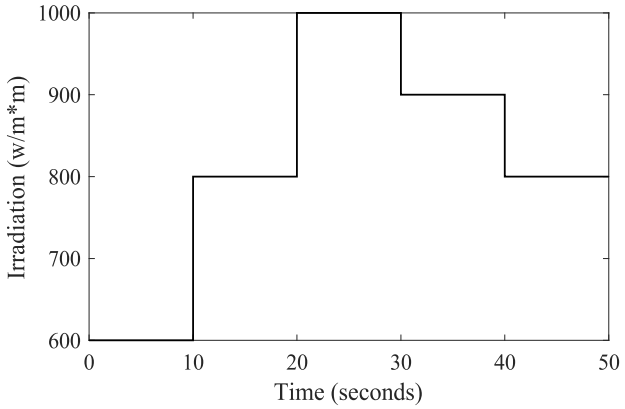

FIGURE 7. Irradiation variation form under a fixed temperature value (T = 25°C).

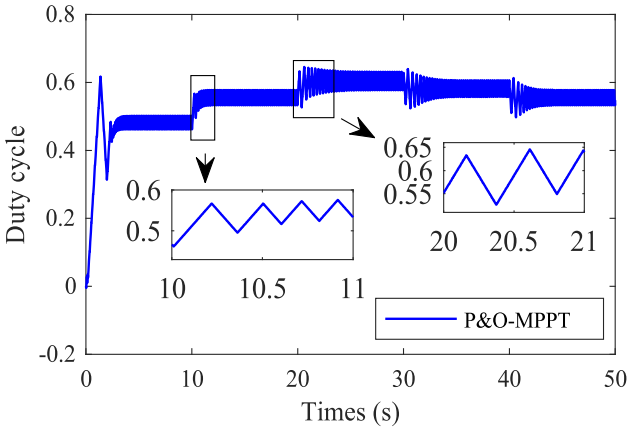

FIGURE 8. Duty cycle evolution for the given irradiation form under the P&O solution.

TABLE 2. Overall parameters for simulation.

DC/DC parameters	
C_{in}	470 μF
C	470 μF
L	1 mH
Switching frequency	50 kHz
PSO parameters	
c_1	1.1
c_2	0.8
w	0.3
N_p	50
ε	0.08
Photovoltaic panel (matrix of Ns and Np cells) parameters	
Maximum power	250 W
Open-circuit voltage(V_{co})	37.85
Short-circuit current (I_{cc})	8.25 (A)
Parallel resistance R_p	1000 (Ω)
Serial resistance R_{se}	0.001 (Ω)
Optimum operating current	8.25 (A)
Optimum operating voltage	31.4 (V)

The influence of the fluctuation in the duty cycle parameter was seen in the voltage and the power output of the PV system, as it is in figure (9). This is very clear at the start of the simulation and in each variation of the irradiation factor. This is due to the instability of duty value. Also, it is verified by the figure (8). These fluctuations, on the duty cycle can be evaluated by different signal decompensation methods, as it is described in those references [29]–[31].

B. MPPT-PSO CONTROL SIMULATION RESULTS

With the previously given form of irradiation (figure (7)), the PSO-MPPT control tool is tested, and the results are given as follow:

Figure (12) illustrates the evolution of the obtained power when the swarms still search for the optimal solution for increasing power. As there are 50 particles and the irradiation factor variation is quick, the stability of the swarms will take more time. Therefore, in figure (12), the electrical power form is not very stable at the beginning of each new irradiation zone. However, at the end of the new irradiation zone, the power starts becoming more stable. This specification is related to the online MPPT-PSO running mode. Refers to these results, the minimum needed time for having a stable particle is 40 seconds. These statistics were depicted after using a calculator which has these specifications (i7, 6 GB Ram, 2.5kHz).

So based on these results, we recommend using the online MPPT-PSO solution only for two conditions: the first one is for the case where the irradiation form is not very quick or for the case, where the used calculator performances are better than used. For this simulation case, the solution is to apply the MPPT-PSO offline and this is searching the optimum solution for each irradiation factor and then store these values. Then, these results will be summarized in a matrix table which gives the best solution for each case. Figure (10), explains the process function.

The offline PSO algorithm running was applied for several irradiation factors to build the MPPT PSO table. The 50 particles evolution was tested for one hundred given calculation iterations and by a random start, the particles' positions into the space of global fitness function value are represented in figure (11). This figure shows four selected iterations for all the particles, and it exposes the position of the particle in the frame of the real fitness function and the previous fitness

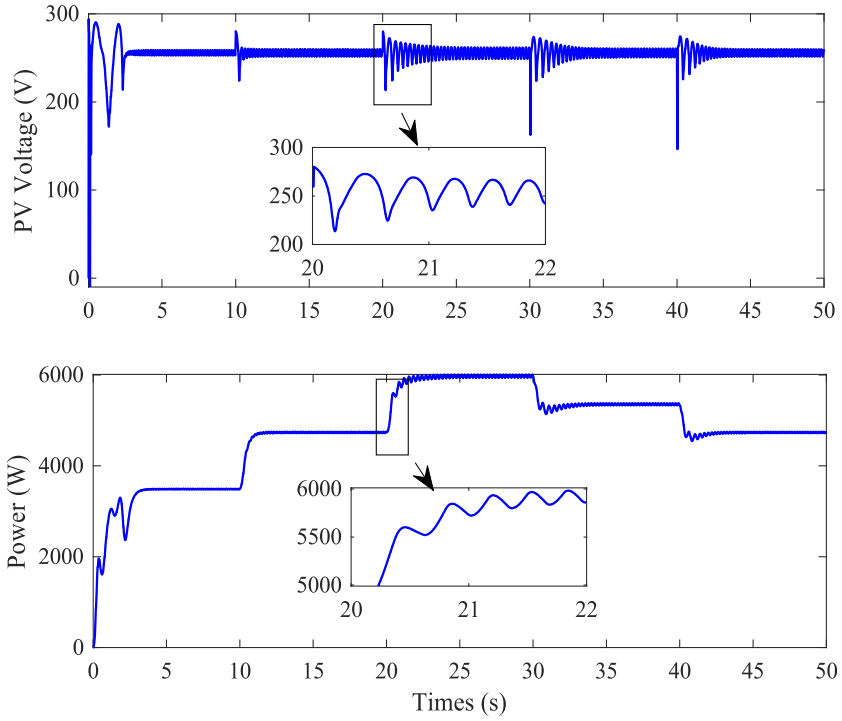

FIGURE 9. Under the P&O solution, according to power and voltage.

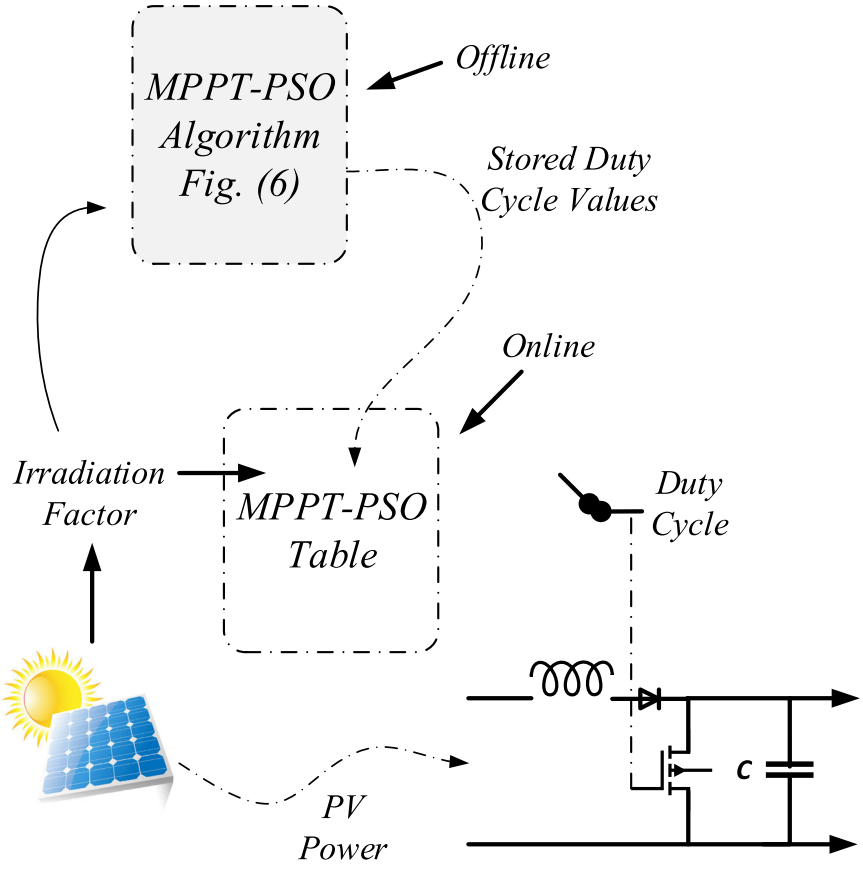

FIGURE 10. After running the MPPT-PSO online, use this method to fix the MPPT-PSO table.

function for each particle. The obtained results show that the algorithm can come to find the best value from the twentieth iteration.

Basing on the PSO results, which are implemented into the MPPT PSO table; the newly obtained power is given as it is in figure (12). The power stability is now clear face the

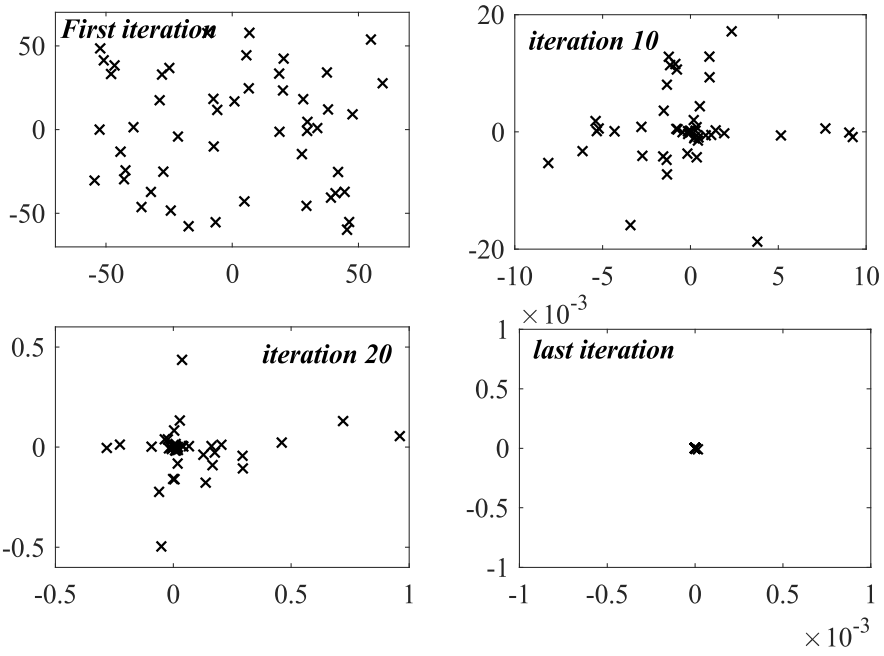

FIGURE 11. Particles evolution into the space of fitness function for one hundred iterations.

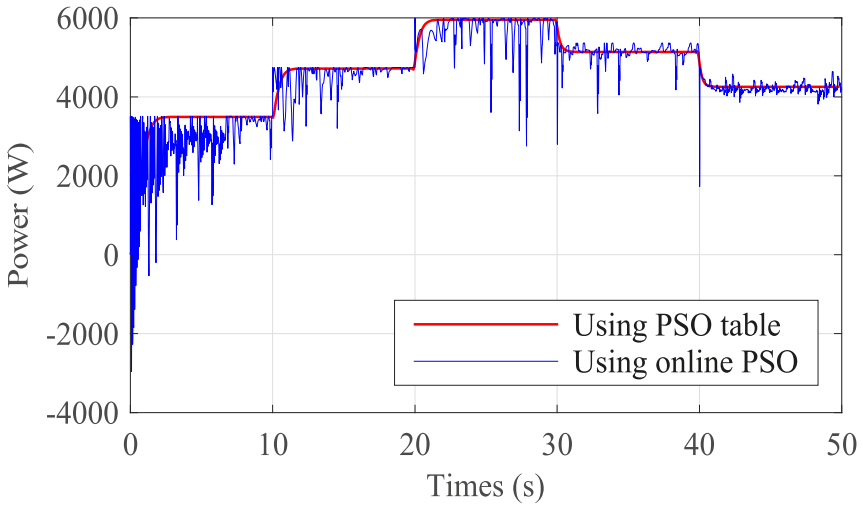

FIGURE 12. Outputted power using an online MPPT-PSO and the MPPT PSO table.

other solution. This stable comportment of power gives better energetic performance if used for charging an electric vehicle.

Actually, the MPPT PSO table contains the output results from the online MPPT-PSO. After running the online MPPT-PSO, all the duty cycles, which correspond to the different radiation form are stored when the outputted PV power come stable. So, these duty cycles, which come from the online MPPT-PSO are inserted into a table, called MPPT-PSO table. This method, will minimize the calculation time when the irradiation parameter changes and help finding the best duty cycle in a less period. This method is very interesting when the vehicle is which a large speed into the city, where the shadow zones are extremely existing. So a quick response will help extract rapidly the solar power, contrary to the online MPPT-PSO, which needs a large time for a stability.

C. RESULTS COMPARISON

At the end of the study, the two results are summarized in table (3), for showing the related statistics in terms of tracking speed, power chattering value. Also, these results were used to estimate the possible gain of energy if using one of the two proposed solar control solutions. This is for all the irradiation zones tested in this work. The PSO-MPPT related results were based on the PSO-MPPT table solution and the online PSO-MPPT method. The global efficiency of the PSO-MPPT solution if using the table method is clear in all

TABLE 3. PSO-MPPT and P&O-MPPT efficiency comparison.

Performance Parameter	*Technique*	*Irradiation*			
		1000	800	600	400
PV power (W)	P&O	5973	4719	3467	2231
	$PSO^{1,2}$	5989	4743	3500	2290
Tracking speed (s)	PSO^{2}	11,578	9,874	7,771	6,695
	P&O	6.177	4.182	3.311	2.793
	PSO^{1}	3.04	2.32	2.09	1.49
Power chattering (W)	P&O	46	20	11	6.1
	PSO^{2}	**Variable between 1000 to 20**			
	PSO^{1}	21	12	7.5	3.2
PSO^{1}: PSO table, PSO^{2}: PSO online, $PSO^{1,2}$ the two PSO methods					

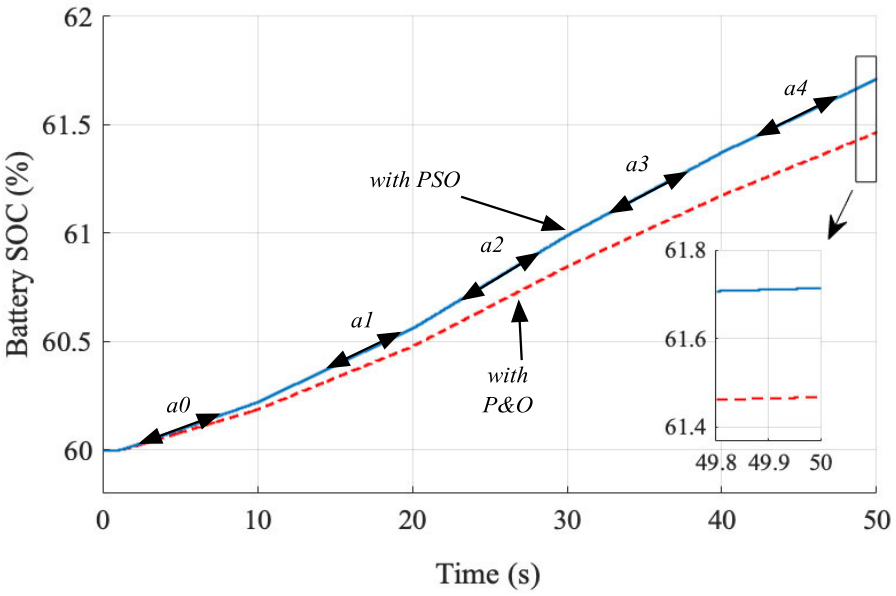

FIGURE 13. Outputted power using an online MPPT-PSO and the MPPT P&O tool.

cases, especially in the electrical power chattering parameter, where the results are the best. Also, the gain of energy can be depicted from this table, which proves that with the PSO solution we can have more power from the solar panel. Even, if using the online PSO solution.

From the other side, the inconvenience of the PSO can be visualized in the tracking speed case, where, more time is needed for having a stable power form.

These results can be proved by the state of charge of the used battery when this solar source was used as one of the main energetic power of the vehicle or when it is used for charging the vehicle. Figure (13) and (14) show the battery state of charge for the case where the vehicle is stopped and when it is in movement with a speed of 60 km/h, respectively These results were depicted for the case of a vehicle based on a pure electric energy source (totally electric vehicle) and for a total charge equivalent to 800 kg with a speed of 60 km/h. It is clear in figure (14), that the battery SOC if using the PSO solution is better, which can give a better autonomy for the vehicle for the case where it is on the road and can decrease the battery charge tile when the vehicle is stopped as it is in figure (13). The influence of irradiation variation can be visualized in figure (13) as it is five different slopes for each case. The irradiation variation can't be visualized for the case where the vehicle is on the road as the battery SOC decrease rapidly due to the energy consumption mode.

As this simulation was applied in 50 seconds, the energetic gain can't be visualized. However, for a real application where the time is unlimited, and the vehicle conduct mode can influence the performance of the PSO solution can be clearer.

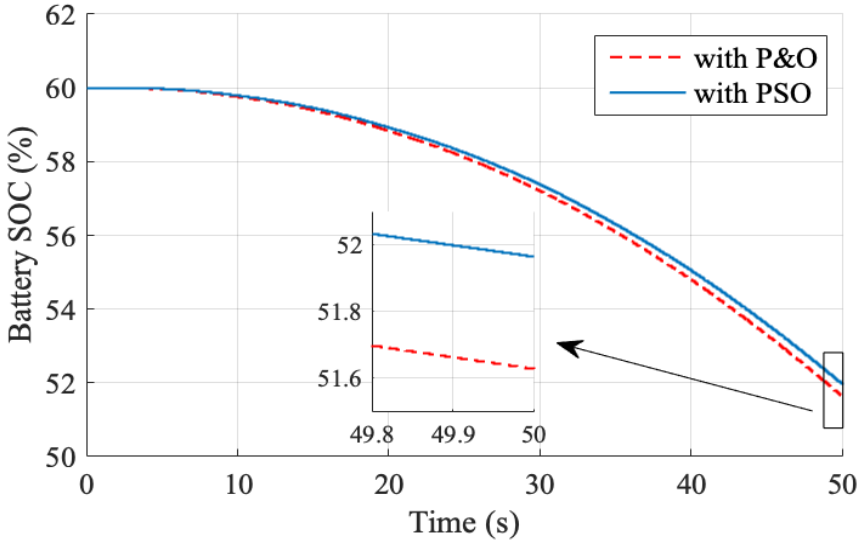

FIGURE 14. Battery SOC for MPPT-PSO and MPPT-P&O cases when the vehicle is in movement with a speed of 60 km/h.

Generally, the PSO solution shows a global best performance and gives better rentability for an electric vehicle application even if it for a partial shading mode. The best performance of the table PSO solution can't be proved if the PSO was not running offline. As these proved advantages of the given solution, the drawbacks can't be hidden. It's related especially to the needed database that must be built before, having the best duty cycle for each irradiation value. This is maybe varied between zone and concerning the weather condition.

VII. CONCLUSION

The goal of the work described in this paper is to improve the efficiency of a photovoltaic (PV) device operated by the MPPT technique to ensure the extraction of the full power supplied by the PV sector. This is to show that the chosen MPPT control solution has an effect on vehicle autonomy when using photovoltaic cells on the car body.

Two control techniques were applied and tested to show the energetic performances and the algorithm rapidity. The MPPT-P&O and the MPPT-PSO are the two used algorithms. When using the first solution, the big shuttering on the given power, especially when the irradiation parameter change, was making the battery charging step more slight and have given less energetic performances. The MPPT-PSO was therefore tested for better global output. As a result, using this approach, energy rentability is improving, but global productivity has declined as the system's rapidity decreases. Thus, using the PSO-MPPT table process, the energy output was reserved and the speed of the calculation processor increased. This has been demonstrated by the results provided in the last section, particularly in relation to the state of charge of the battery.

REFERENCES

[1] C. Mahmoudi, A. Flah, and L. Sbita, "Prototype design of a compact plug-in solar electric vehicle application for smart power management architecture," in *Proc. Int. Conf. Green Energy Convers. Syst. (GECS)*, Mar. 2017, pp. 1–4.

[2] M. B. Ammar, R. B. Ammar, and A. Oualha, "Photovoltaic power prediction for solar car park lighting office energy management," *J. Energy Resour. Technol.*, vol. 143, no. 3, Aug. 2020, Art. no. 031303.

[3] S. V. Verdú, C. S. Blanes, and D. L. Sánchez, "Study of economic feasibility to recharge different types of electric vehicles with photovoltaic solar panels," *J. Sol. Energy Eng.*, vol. 136, no. 4, May 2014, Art. no. 044502.

[4] F. Aymen, M. Alowaidi, M. Bajaj, N. K. Sharma, S. Mishra, and S. K. Sharma, "Electric vehicle model based on multiple recharge system and a particular traction motor conception," *IEEE Access*, vol. 9, pp. 49308–49324, 2021.

[5] J.-J. Hwang, J.-K. Kuo, W. Wu, W.-R. Chang, C.-H. Lin, and S.-E. Wang, "Lifecycle performance assessment of fuel cell/battery electric vehicles," *Int. J. Hydrogen Energy*, vol. 38, no. 8, pp. 3433–3446, Mar. 2013.

[6] A. Esfandyari, B. Norton, M. Conlon, and S. J. McCormack, "Performance of a campus photovoltaic electric vehicle charging station in a temperate climate," *Sol. Energy*, vol. 177, pp. 762–771, Jan. 2019.

[7] A. K. Podder, N. K. Roy, and H. R. Pota, "MPPT methods for solar PV systems: A critical review based on tracking nature," *IET Renew. Power Gener.*, vol. 13, no. 10, pp. 1615–1632, Jul. 2019.

[8] M. Mao, L. Cui, Q. Zhang, K. Guo, L. Zhou, and H. Huang, "Classification and summarization of solar photovoltaic MPPT techniques: A review based on traditional and intelligent control strategies," *Energy Rep.*, vol. 6, pp. 1312–1327, Nov. 2020.

[9] P. Widyantoro, R. Sirait, and A. Musafa, "MPPT system using incremental conductance for solar cell in normal and partial shading conditions," in *Proc. 6th Int. Conf. Electr. Eng., Comput. Sci. Informat. (EECSI)*, Sep. 2019, pp. 352–357.

[10] B. Lahfaoui, S. Zouggar, B. Mohammed, and M. L. Elhafyani, "Real time study of P&O MPPT control for small wind PMSG turbine systems using arduino microcontroller," *Energy Procedia*, vol. 111, pp. 1000–1009, Mar. 2017.

[11] R. Balasankar, G. T. Arasu, and J. S. C. M. Raj, "A global MPPT technique invoking partitioned estimation and strategic deployment of P&O to tackle partial shading conditions," *Sol. Energy*, vol. 143, pp. 73–85, Feb. 2017.

[12] T. Radjai, L. Rahmani, S. Mekhilef, and J. P. Gaubert, "Implementation of a modified incremental conductance MPPT algorithm with direct control based on a fuzzy duty cycle change estimator using dSPACE," *Sol. Energy*, vol. 110, pp. 325–337, Dec. 2014.

[13] H. Renaudineau, F. Donatantonio, J. Fontchastagner, G. Petrone, G. Spagnuolo, J.-P. Martin, and S. Pierfederici, "A PSO-based global MPPT technique for distributed PV power generation," *IEEE Trans. Ind. Electron.*, vol. 62, no. 2, pp. 1047–1058, Feb. 2015.
[14] Y. Wang and Z. Huang, "Optimization-based energy management strategy for a 48-V mild parallel hybrid electric power system," *J. Energy Resour. Technol.*, vol. 142, no. 5, Mar. 2020, Art. no. 052002.
[15] J. Yang, L. He, and S. Fu, "An improved PSO-based charging strategy of electric vehicles in electrical distribution grid," *Appl. Energy*, vol. 128, pp. 82–92, Sep. 2014.
[16] S. A. Oliveira, L. P. Sampaio, F. M. De Oliviera, and F. R. Durand, "A feed-forward DC-bus control loop applied to a single-phase grid-connected photovoltaic system operating with PSO-based MPPT technique and active power-line conditioning," *IET Renew. Power Gener.*, vol. 11, no. 11, pp. 1–19, 2017.
[17] A. R. Bhatti, Z. Salam, M. J. B. A. Aziz, K. P. Yee, and R. H. Ashique, "Electric vehicles charging using photovoltaic: Status and technological review," *Renew. Sustain. Energy Rev.*, vol. 54, pp. 34–47, Feb. 2016.
[18] G. R. Chandra Mouli, P. Bauer, and M. Zeman, "System design for a solar powered electric vehicle charging station for workplaces," *Appl. Energy*, vol. 168, pp. 434–443, Apr. 2016.
[19] F. Mayssa, F. Aymen, and S. Lassaad, "Influence of photovoltaic DC bus voltage on the high speed PMSM drive," in *Proc. 38th Annu. Conf. IEEE Ind. Electron. Soc. (IECON)*, Oct. 2012, pp. 4489–4494.
[20] O. Rabiaa, B. H. Mouna, S. Lassaad, F. Aymen, and A. Aicha, "Cascade control loop of DC–DC boost converter using PI controller," in *Proc. Int. Symp. Adv. Electr. Commun. Technol. (ISAECT)*, Nov. 2018, pp. 1–5.
[21] M. Ahmadi, N. Mithulananthan, and R. Sharma, "A review on topologies for fast charging stations for electric vehicles," in *Proc. IEEE Int. Conf. Power Syst. Technol. (POWERCON)*, Sep./Oct. 2016, pp. 1–6.
[22] F. Aymen, "HEV recharge battery algorithm using a fuzzy controller," in *Proc. Int. Conf. Green Energy Convers. Syst. (GECS)*, Mar. 2017, pp. 1–5.
[23] D. Sandeep, "Electric vehicle battery charging," in *Electric Vehicle Battery Systems*. 2001, pp. 69–91.
[24] J. Su, M. Lin, S. Wang, J. Li, J. Coffie-Ken, and F. Xie, "An equivalent circuit model analysis for the lithium-ion battery pack in pure electric vehicles," *Meas. Control*, vol. 52, nos. 3–4, pp. 193–201, Feb. 2019.
[25] K. N. Mude, "Battery charging method for electric vehicles: From wired to on-road wireless charging," *Chin. J. Electr. Eng.*, vol. 4, no. 4, pp. 1–15, Dec. 2018.
[26] F. Maissa, O. Barambones, S. Lassad, and A. Fleh, "A robust MPP tracker based on sliding mode control for a photovoltaic based pumping system," *Int. J. Autom. Comput.*, vol. 14, no. 4, pp. 489–500, Aug. 2017.
[27] Y. Cao, H. Zhang, W. Li, M. Zhou, Y. Zhang, and W. A. Chaovalitwongse, "Comprehensive learning particle swarm optimization algorithm with local search for multimodal functions," *IEEE Trans. Evol. Comput.*, vol. 23, no. 4, pp. 718–731, Aug. 2019.
[28] W. Hayder, A. Abid, and M. Ben Hamed, "Steps of duty cycle effects in P&O MPPT algorithm for PV system," in *Proc. Int. Conf. Green Energy Convers. Syst. (GECS)*, Mar. 2017, pp. 1–4.
[29] Q. Chen, X. Lang, L. Xie, and H. Su, "Detecting nonlinear oscillations in process control loop based on an improved VMD," *IEEE Access*, vol. 7, pp. 91446–91462, 2019.
[30] Q. Chen, L. Xie, and H. Su, "Multivariate nonlinear chirp mode decomposition," *Signal Process.*, vol. 176, Nov. 2020, Art. no. 107667.
[31] Q. Chen, J. Chen, X. Lang, L. Xie, S. Lu, and H. Su, "Detection and diagnosis of oscillations in process control by fast adaptive chirp mode decomposition," *Control Eng. Pract.*, vol. 97, Apr. 2020, Art. no. 104307.

HABIB KRAIEM received the Ph.D. degree in electrical engineering from the National Engineering School of Gabès, Tunisia, in October 2010. He joined the Department of Electrical, Higher Institute of Industrial Systems Gabès, Tunisia. He is currently with the Department of Electrical Engineering, Faculty of Engineering, Northern Border University, Saudi Arabia. His current research interests include the areas of power electronics, machine drives, automatic control, and renewable energy.

AYMEN FLAH was born in Gabès, Tunisia, in 1983. He received the bachelor's degree in electrical engineering and the M.Tech. degree from the ENIG, Tunisia, in 2007 and 2009, respectively, and the Ph.D. degree from the Department of Electrical Engineering, in 2012. He has academic experience of 11 years. He has published over 40 research articles in reputed journals, and over 40 research papers in international conferences and book chapters. His research interests include electric vehicle, power systems, and renewable energy.

NAOUI MOHAMED was born in Nefta, Tunis, in 1991. He received the degree in electrical engineering from the University of Gabès, Tunisia, in 2015. He is currently pursuing the Ph.D. degree in electrical engineering in the research unit proceeds, energies, environment, and electrical systems, National Engineering School of Gabès. His research interests include electric vehicle, power systems, and renewable energy.

MAJED ALOWAIDI (Member, IEEE) received the B.Eng. degree (Hons.) from the Riyadh College of Technology, in 2006, and the M.A.S. and Ph.D. degrees in computer engineering from the University of Ottawa, in 2012 and 2018, respectively. Since 2012, he has been a member of MCRLAB, University of Ottawa, Canada. He is currently working as an Assistant Professor and the Head of the IT Department, College of Computer and Information Science, Majmaah University, Al Majma'ah, Saudi Arabia. His research interests include cybersecurity, the IoT, semantic web, cloud and edge computing, and smart city.

MOHIT BAJAJ (Member, IEEE) was born in Roorkee, India, in 1988. He received the bachelor's degree in electrical engineering from the FET, Gurukula Kangri Vishwavidhyalya, Haridwar, India, in 2010, and the M.Tech. degree in power electronics and ASIC design from NIT Allahabad, India, in 2013. He is currently pursuing the Ph.D. degree with the Department of Electrical and Electronics Engineering, NIT Delhi, India. He has academic experience of five years. He has published over 30 research articles in reputed journals, international conferences, and book chapters. His research interests include power quality improvement in renewable DG systems, distributed generations planning, application of multi-criteria decision making in power systems, custom power devices, the IoT, and smart grids. He is a member of PES.

SHAILENDRA MISHRA (Senior Member, IEEE) received the M.E. and Ph.D. degrees in computer science and engineering from the Motilal Nehru National Institute of Technology (MNNIT) Allahabad, India, in 2000 and 2007, respectively. He is currently working as an Associate Professor with the Department of Computer Engineering, College of Computer and Information Science, Majmaah University, Al Majma'ah, Saudi Arabia. He has published and presented more than 90 research articles in international journals and more than 90 research papers in international conferences. His recent research interests include the field of cloud and cyber security, SDN, and the IoT security also conducting research on communication system and computer networks with performance evaluation and design of multiple access protocol for mobile communication networks. He is a Senior Member of ACM, and a Life Member of Institution of Engineers India (IEI), the Indian Society of Technical Education (ISTE), and ACEEE.

NAVEEN KUMAR SHARMA (Senior Member, IEEE) received the B.Tech. degree in electrical and electronics engineering from Uttar Pradesh Technical University, Lucknow, in 2008, and the M.Tech. and Ph.D. degrees in power system from the National Institute of Technology Hamirpur, India, in 2010 and 2014, respectively. From March 2014 to May 2017, he worked as a Lecturer with the Department of Electrical Engineering, National Institute of Technology Hamirpur. He is currently an Assistant Professor with the Department of Electrical Engineering, I. K. Gujral Punjab Technical University, Kapurthala, Punjab. He has published several research articles in leading international journals and conference proceedings, and presented papers at several prestigious academic conferences, such as IEEE and Springer. His research interests include the area of power market, renewable energy sources, power system optimization, and condition monitoring of transformers.

SUNIL KUMAR SHARMA received the Ph.D. degree in mathematics from Gautam Buddh Technical University, Lucknow, India. He is currently an Associate Professor of mathematics with the College of Computer and Information Sciences, Majmaah University, Saudi Arabia. His areas of research interest include to deal with the cloud security, mathematical modeling, numerical computation of biomechanics of diarthrodial joints, multicriteria decision model for production systems, robot in the field of education, and cloud security. His current research interest includes mathematical modeling of physical and biological problems in general and mathematical analysis. He is a member of AMC.